

412TW-PA-18339



# RF PLANNING FOR 3D COVERAGE IN CELLULAR LTE RANGE TELEMETRY

4  
1  
2  
T  
W

DAN HARASTY  
ACHILLES KOGIANTIS  
NAN MAUNG  
KIRAN REGE  
ANTHONY TRIOLO

AIR FORCE TEST CENTER  
EDWARDS AFB, CA

NOVEMBER 2018

Approved for public release; distribution is unlimited.  
412TW-PA-18339

412TH TEST WING  
EDWARDS AIR FORCE BASE, CALIFORNIA  
AIR FORCE MATERIEL COMMAND  
UNITED STATES AIR FORCE

<b>REPORT DOCUMENTATION PAGE</b>			<i>Form Approved</i> <i>OMB No. 0704-0188</i>	
Public reporting burden for this collection of information is estimated to average 1 hour per response, including the time for reviewing instructions, searching existing data sources, gathering and maintaining the data needed, and completing and reviewing this collection of information. Send comments regarding this burden estimate or any other aspect of this collection of information, including suggestions for reducing this burden to Department of Defense, Washington Headquarters Services, Directorate for Information Operations and Reports (0704-0188), 1215 Jefferson Davis Highway, Suite 1204, Arlington, VA 22202-4302. Respondents should be aware that notwithstanding any other provision of law, no person shall be subject to any penalty for failing to comply with a collection of information if it does not display a currently valid OMB control number. <b>PLEASE DO NOT RETURN YOUR FORM TO THE ABOVE ADDRESS.</b>				
<b>1. REPORT DATE</b> (DD-MM-YYYY) 25-06-2018		<b>2. REPORT TYPE</b> Technical paper		<b>3. DATES COVERED</b> (From - To) 5-8 November 2018
<b>4. TITLE AND SUBTITLE</b> RF Planning for 3D Coverage in Cellular LTE Range Telemetry			<b>5a. CONTRACT NUMBER</b>	
			<b>5b. GRANT NUMBER</b>	
			<b>5c. PROGRAM ELEMENT NUMBER</b>	
<b>6. AUTHOR(S)</b> Dan Harasty, Achilles Kogiantis, Nan Maung, Kiran Rege, and Anthony Triolo			<b>5d. PROJECT NUMBER</b>	
			<b>5e. TASK NUMBER</b>	
			<b>5f. WORK UNIT NUMBER</b>	
<b>7. PERFORMING ORGANIZATION NAME(S) AND ADDRESS(ES) AND ADDRESS(ES)</b> Perspecta Labs 331 Newman Springs Road Red Bank, NJ 07701			<b>8. PERFORMING ORGANIZATION REPORT NUMBER</b> 412TW-PA-18339	
<b>9. SPONSORING / MONITORING AGENCY NAME(S) AND ADDRESS(ES)</b> 412th Test Wing 195 E Popson Ave Edwards AFB CA 93524			<b>10. SPONSOR/MONITOR'S ACRONYM(S)</b> N/A	
			<b>11. SPONSOR/MONITOR'S REPORT NUMBER(S)</b>	
<b>12. DISTRIBUTION / AVAILABILITY STATEMENT</b> Approved for public release A: distribution is unlimited.				
<b>13. SUPPLEMENTARY NOTES</b> International Telemetering Conference (ITC) Renaissance Glendale Hotel & Spa 9495 West Coyotes Blvd Glendale, AZ 85305, USA				
<b>14. ABSTRACT</b> Initial analysis and lab experiments have provided positive confirmation of the viability of 4G LTE Cellular Technology for Aeronautical mobile telemetry. COTS LTE equipment is deployed for the test range frequency bands. The high speeds of test articles (TAs) can be addressed with a UE add-on applique customized to compensate for the Doppler shifts. The applique has worked effectively with the LTE physical layer. To achieve spectrum efficiency, a multi-cell network is planned. Mobility is managed with native LTE handovers. To address extreme Doppler cases, additional support is provided to mobility management via a central entity that estimates the TA's trajectory and issues handover commands. Within this framework we present aspects of an RF planning study covering the air space around the Edwards Air Force base. The analysis is conducted with a custom RF planning tool to assess signal strength, interference and achievable rates from a placement of cells at various locations in the test range, with antenna pointing that is relatively restricted. Results cover eNB density, antenna pointing strategies, backhaul needs, achievable rates, and multi-user aspects.				
<b>15. SUBJECT TERMS</b> Telemetry, 4G LTE, Doppler				
<b>16. SECURITY CLASSIFICATION OF:</b> Unclassified			<b>17. LIMITATION OF ABSTRACT</b> None	<b>18. NUMBER OF PAGES</b> 11
<b>a. REPORT</b> Unclassified	<b>b. ABSTRACT</b> Unclassified	<b>c. THIS PAGE</b> Unclassified		
			<b>19b. TELEPHONE NUMBER</b> (include area code) 661-277-8615	

# **RF Planning for 3D coverage in Cellular LTE Range Telemetry**

Dan Harasty, Achilles Kogiantis, Nan Maung, Kiran Rege and  
Anthony Triolo

Perspecta Labs

331 Newman Springs Road, Red Bank, NJ 07701

[dharasty, akogiantis, nmaung, krege, atriolo]@perspectalabs.com

## **ABSTRACT**

Initial analysis and lab experiments have provided positive confirmation of the viability of 4G LTE Cellular Technology for Aeronautical mobile telemetry. COTS LTE equipment is deployed for the test range frequency bands. The high speeds of test articles (TAs) can be addressed with a UE add-on applique customized to compensate for the Doppler shifts. The applique has worked effectively with the LTE physical layer. To achieve spectrum efficiency, a multi-cell network is planned. Mobility is managed with native LTE handovers. To address extreme Doppler cases, additional support is provided to mobility management via a central entity that estimates the TA's trajectory and issues handover commands. Within this framework we present aspects of an RF planning study covering the air space around the Edwards Air Force base. The analysis is conducted with a custom RF planning tool to assess signal strength, interference and achievable rates from a placement of cells at various locations in the test range, with antenna pointing that is relatively restricted. Results cover eNB density, antenna pointing strategies, backhaul needs, achievable rates, and multi-user aspects.

## **1. INTRODUCTION**

Implementation of Airborne Mobile Telemetry (AMT) using a cellular network based on the 3GPP LTE standard offers a number of benefits. Given the availability of inexpensive and reliable COTS base-station equipment and mobile devices, it should lead to a substantial reduction in capital and operational expenses. It would also enable the implementation next-generation applications and services in view of the sophistication and feature-richness of these devices that could potentially replace the current equipment that has been in place for several years. Another major benefit would be the elimination of the need for the complex scheduling that the current system requires, [1]. While all of these benefits are certainly attractive to the system administrators, one would not be able to realize them unless a couple of critical issues are successfully resolved: The first issue concerns the high Doppler shifts experienced by the uplink and downlink communications between the Test Articles (TAs) and their serving base stations, while the second involves network planning. As described in [2], the first problem can be successfully overcome by introducing a Doppler estimator/compensator at the mobile transceiver. In this paper, we address the second problem, i.e. that of network planning for AMT.

Note that in a telemetry system based on a cellular network, the base station antennas are fixed; they do not track the TAs they are communicating with. Thus, the air-space in which the TAs move about during various tests needs to be adequately covered by the antenna patterns associated with the base stations to ensure that the TAs can maintain adequately strong communication links throughout their flights. Since this air-space is 3-dimensional, the network planners need to consider 3-dimensional coverage to ensure adequate performance. This is rather different from commercial network planning where the planners essentially deal with 2-dimensional coverage issues.

In the next section, we present an analysis of test-range coverage issues using idealized assumption. In the section that follows, we present a coverage analysis of the air space around the Edwards Air Force Base using a custom tool. Finally, we conclude this paper with a summary of our findings in the last section.

## 2. AIR SPACE COVERAGE – AN IDEALIZED ANALYSIS

We assume the air space of interest to be a prism with a square base aligned with the North-South and East-West directions, where the sides of the base are  $L$  km, and the height is  $H$  km. Radio coverage for this air space is to be provided with  $N^2$  cell sites placed on the square base as shown in fig. 1 below. Thus, the inter-site distance (ISD) is  $d = L/N$  km.

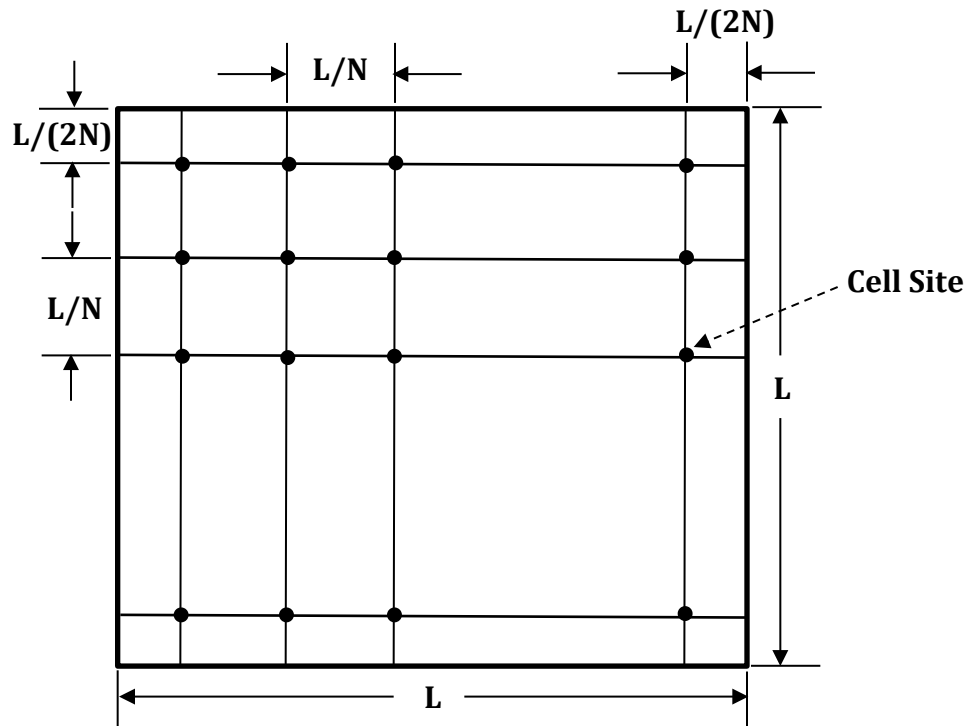


**Fig. 1: Layout of Cell Sites on the Square Base of the Air Space**

Each cell site is divided into four sectors, with each sector served by an antenna system. In LTE parlance, each sector is an LTE cell. We consider two different orientations of the sectors and the corresponding antennas. In Orientation 1, the azimuth directions of the

antenna beams of the four sectors within a cell site are: North, West, South and East. In Orientation 2, they point in the directions: Northeast, Northwest, Southwest and Southeast. The angle of elevation for all antenna beams is:  $\tan^{-1}\left(\frac{H\sqrt{2}}{d}\right)$  Fig. 2 illustrates these antenna/sector orientations in the azimuth plane.

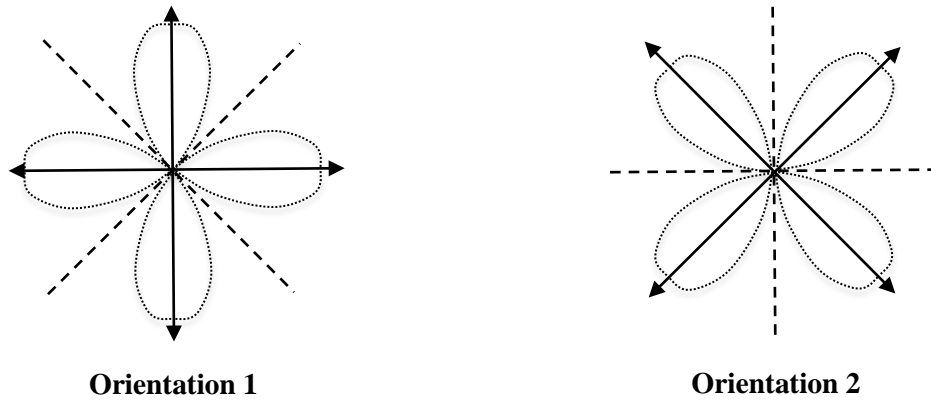


**Fig. 2: Illustration of Antenna/Sector Orientations**

At each cell site, the antennas and sectors can be placed according either of the two orientations shown in fig. 2. We consider three placement patterns: In Placement Pattern 1, the antennas and sectors at all cell sites are placed in accordance with Orientation 1; in Placement Pattern 2, the antennas and sectors at all cell sites are placed in accordance with Orientation 2, whereas in Placement Pattern 3, antennas and sectors at alternate cell sites follow Orientations 1 and 2. Fig. 3 below is an illustration of Placement Pattern 3.

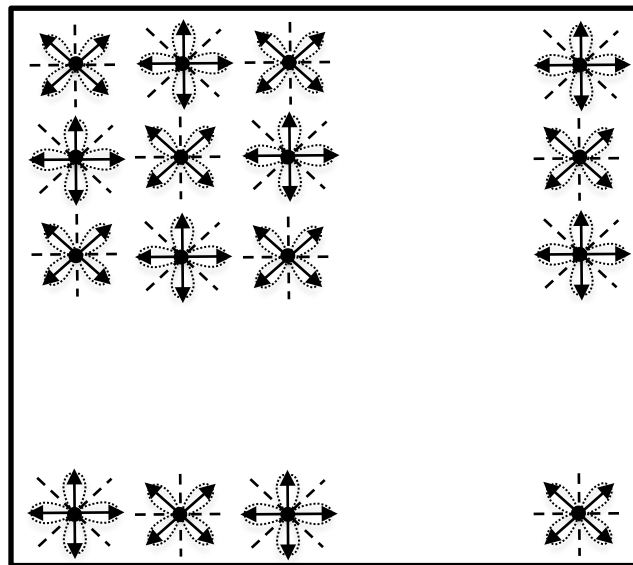


**Fig. 3: Illustration of Placement Pattern 3**

In order to quantify coverage of the air space, we need the antenna gain pattern (beam-shape) and the per-cell transmit power in addition to the location of the cell sites and the orientation of antennas at each of them. We assume that the antenna gain,  $g(\theta)$ , is given by:

$$g(\theta) = \max\left(g_{min}, G - 3.0 * \left(\frac{\theta}{\theta_{3dB}}\right)^2\right) dB, \quad (1)$$

where  $G$  is the maximum antenna gain,  $\theta_{3dB}$  is half of the 3-dB beamwidth of the antenna,  $\theta$  is the angle (in the 3-dimensional space) between the vector pointing from the antenna to the TA and the boresight vector associated with the antenna, and  $g_{min}$  is the floor on the antenna gain that represents the gain associated with leakage outside of the desired beam of the antenna. The receiver antenna at the TA is assumed to be omnidirectional with a 0 dB gain.

Since there is little multipath phenomenon in the wireless channel between the base stations on the ground and airborne TAs, we assume the path-loss characteristics to be based on the inverse-square law. Specifically, the relationship between the base station transmit power from a cell and the received power at the TA is given by:

$$p_R = p_T + g(\theta) - 96.8 - 20 \log_{10}(d_{TA}), \quad (2)$$

where  $p_T$  and  $p_R$  respectively denote the transmit and received powers (both expressed in dBW),  $g(\theta)$  is the antenna gain of the base station transmit antenna as defined in (1) and  $d_{TA}$  is the distance between the base station and the TA.

### Coverage Simulations:

We assume the air space dimensions to be 200 km x 200 km x 15 km. That is,  $L$ , the length and the width of the square base, is 200 km; and  $H$ , the maximum altitude for a TA is 15 km. Within this air space, we quantify the coverage and Doppler performance at four different altitudes: 1 km, 5 km, 10 km and 15 km. At each altitude, we characterize performance using a Monte Carlo method. Thus, keeping the altitude  $h$  fixed at one of these levels, we “drop” the TA randomly within the 200 km x 200 km slice of the air space at a height of  $h$  km from the ground. The TA is assumed to be flying in the horizontal plane, with its heading selected randomly between 0 and 360 degrees. The speed of the TA is  $v$ , which is a simulation parameter. Further, we assume that besides the cell serving the TA, there are  $M$  active cells causing interference to the TA. This is equivalent to assuming that there are  $M$  other TAs within the air space, each of which is being served by a cell other than the one serving the desired TA. Thus, the signal power for the desired TA comes from its serving cell while the interference comes from the  $M$  interfering cells. Consequently, the SINR for the desired TA is given by:

$$SINR = \frac{p_0}{(\sum_{m=1}^M p_m + N_0)}, \quad (3)$$

where  $p_0$  denotes the TA’s received power from the serving cell, for  $m = 1, 2, \dots, M$ ,  $p_m$  denotes the interference power the TA receives from the  $m^{th}$  interfering cell, and  $N_0$  denotes the thermal noise power. Note that all powers in (3) are expressed in the linear, not dB, domain.

For a signal received from cell  $m$ , the Doppler shift experienced by the TA is given by:

$$f_D = (f_c v/c)\cos(\theta_m), \quad (4)$$

where  $f_c$  is the carrier frequency associated with the transmitted signal,  $c$  is the speed of light, and  $\theta_m$  is the angle (in the 3-dimensional space) between the direction in which the TA is flying and the pointing vector from the TA to cell  $m$ . For each of the four altitude levels we repeat this experiment  $K$  times, to generate  $K$  i.i.d. samples. The metric we use to assess the coverage impact of different parameters is the user rate. That is, the bit rate a user can receive under idealized conditions given its SINR. We use the Shannon formula to estimate the user rate  $R$ :

$$R = W \log_2(1 + \text{SINR}), \quad (5)$$

where the SINR is expressed in linear (not dB) units.

We use this method to study the impact of different parameters on the coverage impact of different parameters. Specifically, we characterize the impact of base station density (expressed in terms of the parameter  $N$ ), base station placement pattern, and TA altitude. For coverage performance, we assume that the mobile device at the TA is connected to the base station corresponding to the highest received signal power.

Figure 4 shows the impact of the base station placement pattern on the coverage performance of the air space. Specifically, it shows user rate distributions for the three base station placement patterns at TA altitude of 1 km and 5 km. The parameter  $N$  characterizing the base station density was held fixed at 10 so that the air space was covered by 100 base stations (400 cells) in all cases.

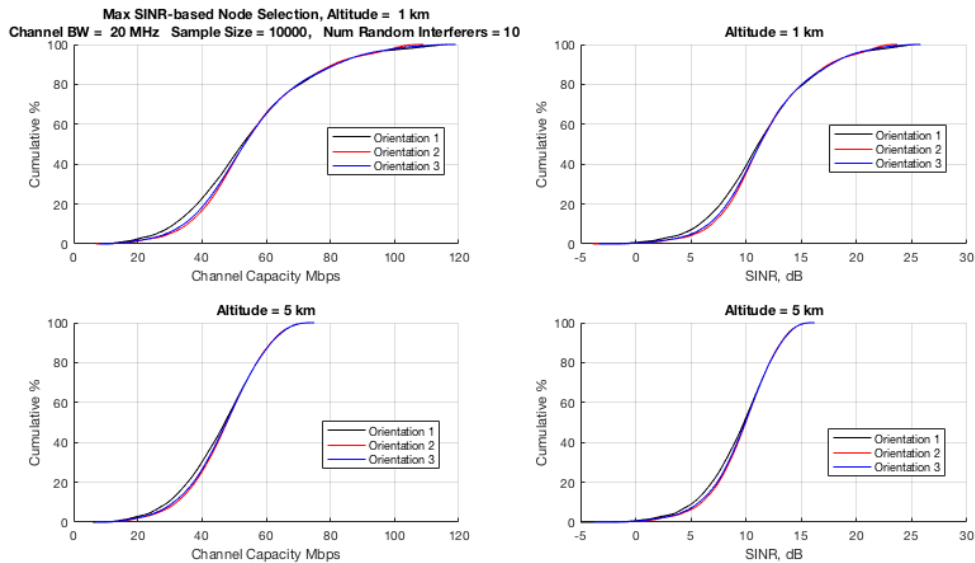


**Figure 4: Impact of Base Station Placement Pattern on Coverage Performance**

As one can see in Figure 4, there is little difference in the coverage performance of the three base station placement patterns considered here. Therefore, in the rest of the study, we only consider Placement Pattern 3 as shown in Figure 3.

Figure 5 shows the impact of altitude on the user rate distribution. Here, the base station density parameter  $N$  was held constant at 10 and Placement Pattern 3 was used in all simulations. Four TA altitudes were considered: 1 km, 5 km, 10 km, and 15 km.

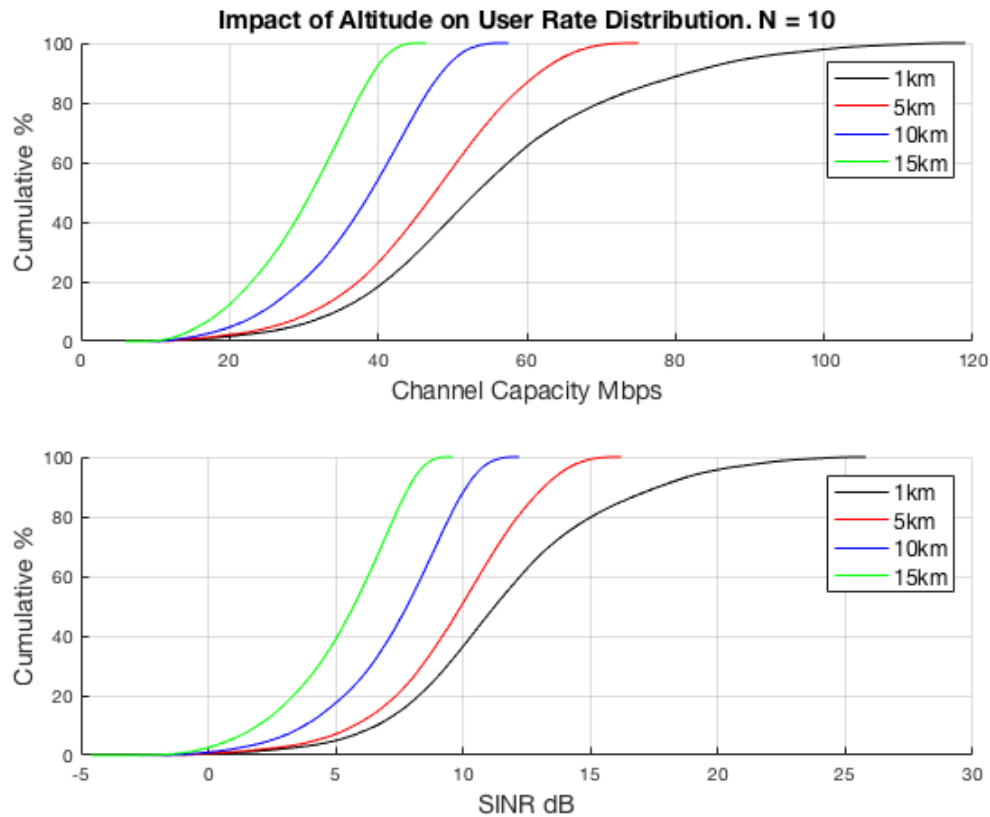


**Figure 5: Impact of TA Altitude on User Rate Distributions**

It is clear from this figure that although the base station antennas pointed up (at the corner of each sector), the highest user rates typically correspond to lower altitudes. The main reason for this seems to be that since the base stations themselves are at ground level, the path loss to lower altitudes tends to be lower (on an average) than at higher altitudes.

Figure 6 shows the impact of density on the coverage performance of the air space. Specifically, it shows the user rate distributions for TA altitudes 1 km and 15 km for three values of the base station density parameter  $N$ , namely, 5, 10 and 20.



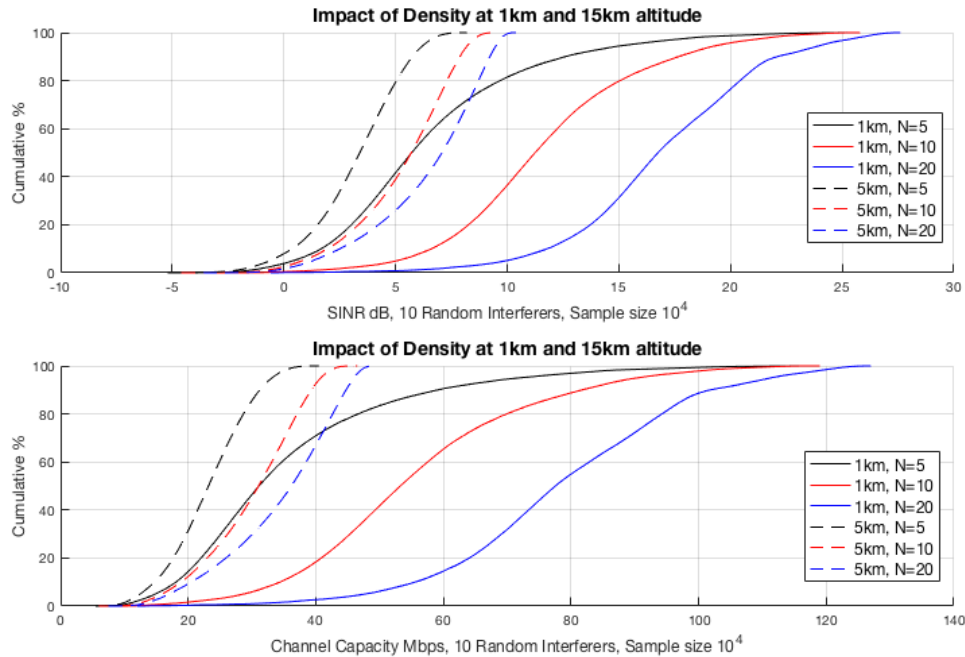


**Figure 6: Impact of Base Station Density on Coverage Performance**

It is clear from Figure 6 that increasing the base station density typically leads to improved coverage, i.e. higher user rates. However, one can see a trend of diminishing returns here: While there is a large improvement in user rates when the parameter  $N$  is increased from 5 to 10 (i.e. reducing the inter-site distance from 40 to 20 km), increasing  $N$  further to 20 (i.e. reducing the inter-site distance to 10) leads to smaller increases in user rates. The optimal base station density will typically be determined by a compromise between coverage needs (expressed in terms of lower percentiles of user rates) and the economic cost of deploying additional base stations and the associated infrastructure.

The coverage analysis presented so far focused on the user rate distributions under the assumption that the user device is connected to the strongest base station. What has been ignored in this analysis is the Doppler shift experienced by the receiver, which is also critical to the overall system performance. Figures 7a and 7b given below respectively display the user rate distributions and Doppler shift distributions for the default strategy where the user device is connected to the strongest base station and the alternate strategy where it connects to the lowest Doppler base station among all those with SINR of at least  $\theta$  dB. If none of the base stations yields an SINR of  $\theta$  or more, the user device connects to the strongest base station. The base station density parameter  $N$  was 10, and the altitude was 5 km in all cases. The SINR Threshold used in the simulation for 7b was 5 dB.

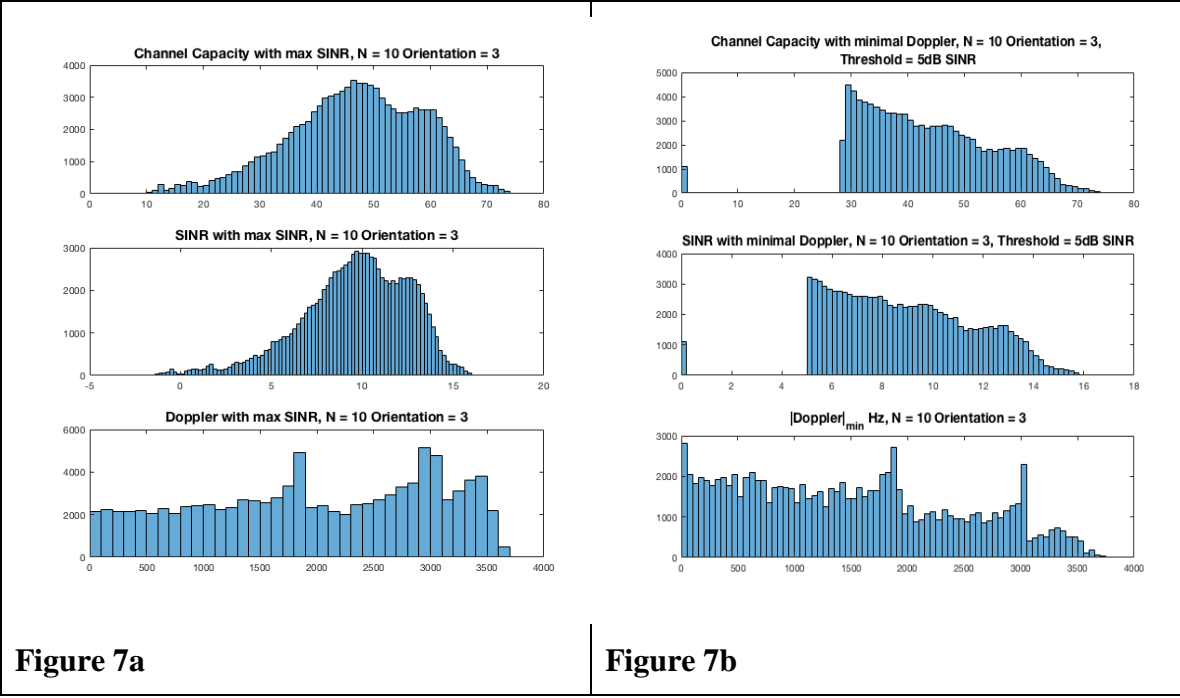


Figure 7a

Figure 7b

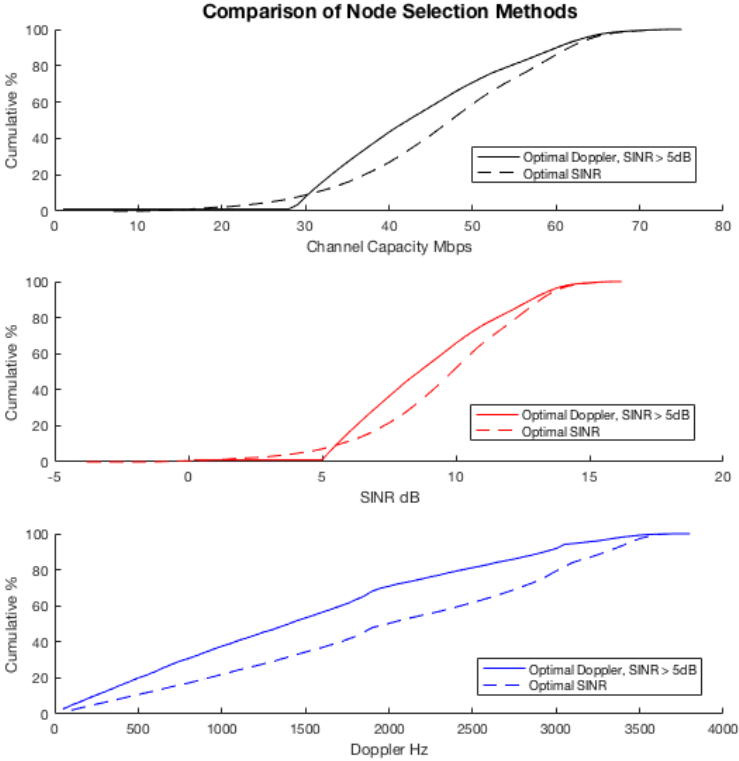
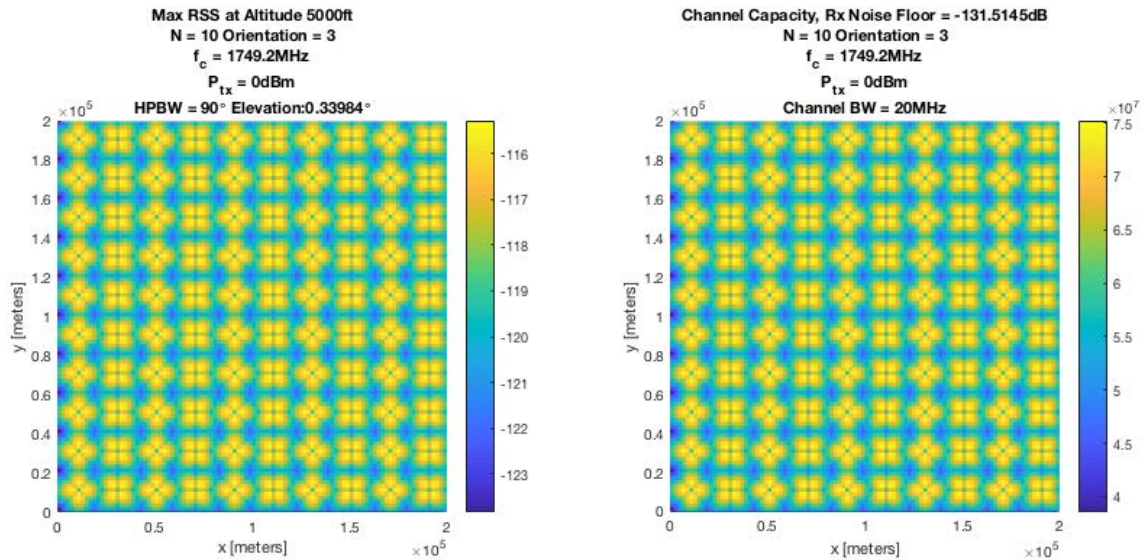


Figure 7c. Comparison of Cell Selection Methods in 7a and 7b

An alternative view of the received signal strength (RSS) heatmap at an altitude of 5000ft is given in Figure 8. The elevation is somewhat low so that the antenna beam pattern

effects can be distinguished. At higher elevations the heatmap become more uniform as the contributions from each and every base station are evenly distributed across the plane.



**Figure 8. Heatmap of Received Signal Strength at given elevation, N=10**

#### 4. SUMMARY

RF planning analysis was conducted for covering a three-dimensional prism space with base stations on the ground to deliver sufficient data rates to test articles that are airborne at various altitudes. The analysis pointed to the dependency on base station separation rather than the pointing arrangement as a more determining factor in achieving higher data rates delivered. The link quality was quantified and assessed to be deteriorating at higher altitudes due to interference and larger link distance. A trade off analysis of link quality distribution over base station to base station distance also indicates that very large spacing produces diminishing returns.

#### 4. REFERENCES

- [1] Achilles Kogiantis, Kiran Rege, Anthony A. Triolo, "LTE System Architecture for Coverage and Doppler Reduction in Range Telemetry," *International Telemetry Conference (ITC 2017)*, Las Vegas, NV, November 2017
- [2] Eddie Fung, William H. Johnson, Achilles Kogiantis, Kiran M. Rege, "Doppler Estimation and Compensation for LTE-Based Aeronautical Mobile Telemetry," *International Telemetry Conference (ITC 2018)*, Scottsdale, AZ, November 2018.

#### Acknowledgement

Effort sponsored by the U.S. Government under Other Transaction number W15QKN-15-9-1004 between the NSC, and the Government. The US Government is authorized to reproduce and distribute reprints for Governmental purposes notwithstanding any copyright notation thereon.